Technical article

Paradoxes of Homogenization

Abstract — **The Compumag Community is quite familiar with multiscale analysis and simulation – multigrid methods, multiphysics, homogenization. The latter is a two-scale problem with special physical and mathematical significance; a fine-scale heterostructure is to be replaced with an equivalent homogeneous one. Clearly, this simplification can be conducive to analytical and numerical studies, as long as the word "equivalent" is given a meaningful and unambiguous definition.**

This article includes a brief review of effective medium theories (homogenization) for electromagnetic fields in periodic structures, but the focus is on *paradoxes* of homogenization.

First, there may appear to be *incompatible symmetries* between the scattering characteristics of a fine-scale heterostructure and the respective homogenized sample. Indeed, the former may lack mirror symmetry, while the latter by necessity is geometrically symmetric. It turns out, however, that this lack of symmetry can be accurately rendered on the coarse scale if the homogenized model includes magnetoelectric coupling.

Second, as the number of layers in a periodic heterostructure is increased from one to two to three, etc., one intuitively anticipates a gradual transition of electromagnetic parameters to their bulk values. Paradoxically, there is in fact no such transition; in a sense, one layer is already "bulk".

Finally, the article reflects on a curious case of "effective medium transformation". For laminated magnetic cores, typical in electric machines and devices, the physical and mathematical nature of the model changes upon homogenization. The eddy current problem on the fine scale becomes – not by design but by necessity – a magneto-quasistatic problem on the coarse scale.

The article is based on the author's joint work with Vadim Markel, Shahriyar Hossain, Markus Schöbinger, Karl Hollaus, and Yidong Chong.

I Warm-Up: Good or Poor Conductors for Low Loss?

Even though this "warm-up" section is only loosely related to the remainder of the article, I hope it will be of interest in its own right.

Let us recall that in a lossy material with a scalar dielectric permittivity ϵ' and conductivity σ, the Maxwell curl-**H** equation is, in the SI system,

$$\nabla \times \mathbf{H} = \mathbf{J} + \partial_t \mathbf{D} = \sigma \mathbf{E} + \partial_t(\epsilon' \mathbf{E}) \tag{1}$$

In the frequency domain, under the $\exp(-i\omega t)$ phasor convention, the right hand side gets expressed in terms of the complex permittivity $\epsilon = \epsilon(\omega) = \epsilon'(\omega) + i\epsilon''(\omega)$:

$$\nabla \times \mathbf{H} = -i\omega\epsilon\mathbf{E}, \qquad \epsilon = \epsilon' + i\epsilon'', \quad \epsilon'' \stackrel{\text{def}}{=} \frac{\sigma}{\omega} \tag{2}$$

(the frequency dependence of ϵ is not explicitly indicated for brevity).

It is common knowledge that electric power transmission and consumption relies on *good conductors* (such as copper or aluminum) – that is, materials with a high conductivity, $\sigma \gg \omega\epsilon'$, or equivalently[1]

$$|\epsilon''| \gg \epsilon' \qquad \text{(power applications)} \tag{3}$$

Highly conductive materials in electric power applications minimize losses. This observation appears obvious and unremarkable, until a comparison is drawn with applications in optics and photonics, where the use of good conductors (e.g. gold or silver) leads to *higher* losses. The desirable relation therefore is

$$|\epsilon''| \ll \epsilon' \qquad \text{(optics and photonics)} \tag{4}$$

In the area of plasmonics in particular, it is usually desirable to reduce losses and use materials with a small imaginary part of the dielectric permittivity [47].

It is patently obvious that the low-loss conditions in optical vs. traditional electrical applications are diametrically opposite; but a fundamental question is: Why?

The first inclination may be to appeal to frequency differences, but conditions (3), (4) are frequency independent. I invite the reader to find a more credible explanation. For my own take on that, see [96].

II Compumag: Multiscale and Two-Scale Problems

For several decades, the Compumag community has intensively studied multiscale methods and their applications to electromagnetic analysis: various versions of multigrid methods, multiphysics problems, finite element methods (FEM) with *hp*-refinement, finite difference (FD) – Trefftz schemes ("FLAME"), Finite Integration Techniques (FIT), a large variety of effective medium theories, and more [6,7,10–12,15,18–20,22,25–30,32–36,41,43,49,51,59,62,68–70,72–76,81,82,84,99–103]. The applications have included eddy current problems in electric machines and devices, magnetic composites, laminated cores, granular materials, windings, Litz wires, geophysical problems, carbon fiber reinforced polymer composites, spatial charge distribution in particle accelerators, simulations of colloidal particles, photonic crystals, open-boundary problems in geophysics.

The collective effort to create and validate benchmark problems in the TEAM workshop deserves a special separate mention; see e.g. [15,41].

The reference list above is representative but certainly far from complete. It is colored by my own research experience and may serve as a starting point for further literature search by the interested reader. It is clear at the same time that most of Compumag-related research revolves around low-frequency applications: eddy currents, electrical machines, quasistatic problems. The present article, in contrast, deals with *wave propagation* in complex

[1] The absolute value for $|\epsilon''|$ is used to make the expression meaningful for the $\exp(+i\omega t)$ phasor convention as well. The ratio $|\epsilon''|/\epsilon'$ is the standard loss tangent.

media, such as metamaterials and photonic crystals – artificial periodic structures judiciously designed to engender non-trivial physical effects such as negative refraction, high absorption, lensing, beam steering, and more.[2]

An analysis of existing effective medium theories is given in our prior publications [39,94,98], [95, Chapter 9]. Here, I focus not on these theories *per se* but rather on general paradoxes of homogenization. These paradoxes have to do with essential yet counter-intuitive features of wave propagation in fine-scale heterostructures.

Homogenization is, typically, a two-scale rather than a multiscale problem. A fine-scale heterostructure is to be replaced with an equivalent homogeneous sample. Without an unambiguous definition of the word *equivalent*, this task is imprecise. In the physics literature, theoretical analyses typically involve volume averaging (or, in some cases, boundary averaging) of fine-scale fields, leading to their coarse-grained counterparts. This approach, however, is not as natural and straightforward as it appears at first glance.

Indeed, let us first note that coarse-grained fields inside fine-scale structures do not physically exist. In their venerable book, Penfield & Haus write [71, pp. 42–43]:

> We now indicate why fields inside materials are impossible to measure.... within the polarized body the fields **E** and **H** are mathematical constructs defined in terms of equivalent smoothed charge and current distributions. A measurement of an electric or magnetic field inside the polarized body would not necessarily measure these fields because the spatial and time averages taken by a probe, such as an energetic electron beam shot through the body or electrons of a conduction current, are not necessarily the same as the averages implied in [macroscopic Maxwell's equations]. ... the fields predicted from [macroscopic Maxwell's equations] have physical meaning only in the space surrounding a polarized body or in slots cut into the body for the purpose of measuring the fields but have no direct physical meaning inside the body itself.

Secondly, it can be argued (I believe, convincingly) that the goal of homogenization is to accurately render the *macroscopic measurable fields* around a given heterostructure. It is in that sense that equivalence between fine- and coarse-scale structures is to be understood. A technical definition is given in our prior publications [39,94,98] and is summarized in Section D (p. 4). The focus of this article, though, is not on effective medium theory *per se*, but rather on *paradoxes of homogenization*.

Three such paradoxes are reviewed. One of them concerns homogenization of structures lacking mirror symmetry. Once such a structure is replaced with a homogeneous one, it appears that the asymmetry is lost and cannot be recovered. We have shown,[3] however, that a nonsymmetric structure can in fact be accurately homogenized if the model includes magnetoelectric coupling (Section V).

It is commonly assumed that, as the thickness of a finite-size heterostructure is gradually increased from one layer to 2, 3, ... layers, a transition to bulk material characteristics takes place. This assumption gives rise to our second paradox: we claim[4] that *for periodic structures* there is no such transition: in a sense, one layer is already "bulk" as far as homogenization is concerned (Section VI).

Finally, there is a peculiar case of "effective medium transformation"; it involves laminated magnetic cores – stacks of insulation-coated thin sheets of steel. (The insulation reduces eddy currents and losses.) The eddy current problem, with the displacement currents neglected, applies on the fine scale; but on the coarse scale the physical and mathematical nature of the problem changes: it becomes quasi-magnetostatic (Section VII).[5]

III Preliminaries

As in [60, 94, 98], we consider homogenization of periodic heterostructures characterized by the intrinsic scalar permittivity $\tilde{\epsilon}(\mathbf{r})$. The tilde sign is used for all lattice-periodic quantities. The individual constituents of the structure are assumed to be linear, local and intrinsically nonmagnetic. The effective parameters, to be defined, are denoted by ϵ_{eff} and μ_{eff} and are in general second-rank tensors different from unity. We will also include into consideration the effective parameters of magnetoelectric coupling χ_{eff} and ζ_{eff}. The complete effective material tensor $\mathcal{M}$, relating the ($\mathbf{D}$, $\mathbf{B}$) field pair to ($\mathbf{E}$, $\mathbf{H}$), is represented by a matrix

$$\mathcal{M} \equiv \begin{pmatrix} \epsilon_{\text{eff}} & \chi_{\text{eff}} \\ \zeta_{\text{eff}} & \mu_{\text{eff}} \end{pmatrix} \tag{5}$$

The dimension of $\mathcal{M}$ is in general 6×6 but can be reduced in special cases, such as 2D problems of s or p polarization.

Bloch-periodic functions (Bloch waves) are written in the following generic form:

$$f(\mathbf{r}) \;=\; \tilde{f}(\mathbf{r}) \exp(i\mathbf{q}\cdot\mathbf{r}) \;, \tag{6}$$

where $\mathbf{q}$ is the Bloch wave vector. In the case of orthorhombic lattices, the lattice periodicity is expressed as

$$\tilde{f}(x+a_x, y+a_y, z+a_z) = \tilde{f}(x,y,z) \;, \tag{7}$$

where a_x, a_y and a_z are the lattice periods, and all points are simultaneously located within the heterostructure.

Fine-level fields – that is, the exact solutions to the macroscopic Maxwell's equations – are denoted by small letters $\mathbf{e}$, $\mathbf{d}$, $\mathbf{h}$ and $\mathbf{b}$. These fields are assumed to be subject to the following constitutive relations:

$$\mathbf{d}(\mathbf{r}) \;=\; \tilde{\epsilon}(\mathbf{r})\,\mathbf{e}(\mathbf{r}) \;, \quad \mathbf{b}(\mathbf{r}) \;=\; \mathbf{h}(\mathbf{r}) \tag{8}$$

We adopt the $\exp(-i\omega t)$ phasor convention at a given frequency ω. The free-space wavenumber and wavelength are

$$k_0 = \omega/c; \quad \lambda = 2\pi/k_0 \tag{9}$$

IV Effective Medium Theories in Physics and Mathematics

In physics, effective medium theories date back to the work of Mossotti (1850), Lorenz (1869), Lorentz (1878), Clausius

[2] Some of our peers inside and outside the Compumag community equate metamaterials with double-negative (or negatively refracting) materials. I believe that such a definition is way too narrow and that most experts in metamaterials research would not adopt it; there are many interesting phenomena besides negative refraction.

[3] This is joint work with Shahriyar Hossain and Yidong Chong [97].

[4] This is joint work with Vadim Markel and Shahriyar Hossain [37].

[5] This is joint work with Marcus Schöbinger and Karl Hollaus [85].

(1879), and Maxwell Garnett (1904). A number of more advanced studies followed, of which most relevant to electromagnetics are various extensions of the Maxwell Garnett formula to wave problems: by Lewin (1947), Khizhnyak (1957–59), Waterman & Pedersen (1986) [45, 46, 55, 104]. In particular, Khizhnyak made an interesting observation that "an artificial dielectric ... made from inherently nonmagnetic materials, at higher frequency ... will exhibit both dielectric and magnetic anisotropy;" see [66] for an interesting summary of these developments. Modern physical theories of homogenization are presented in Choy's monograph [17], with the emphasis on random rather than periodic media.

The mathematical literature on the subject is also rich and includes the monographs by Bakhvalov & Panasenko, Bensoussan *et al.*, Oleinik and her collaborators, Dal Maso, Sanchez-Palencia and Tartar [3, 5, 42, 83, 92].

Various numerical approaches to homogenization have also been put forward within the multiscale framework that has progressed from multigrid / multilevel methods in the 1960s–1980s to multiphysics [1, 21, 24, 40, 67].

Many existing theories operate in the *homogenization limit*, when the cell size of the microstructure (or another similar parameter) tends to zero. This is sufficient for many applications, but not for all. One notable exception is optical metamaterials – artificial periodic structures judiciously designed to control the propagation of electromagnetic waves and to achieve remarkable effects such as high-frequency magnetism nonexistent in natural materials. If the zero-cell-size limit is taken, magnetism (and negative refraction, an even more remarkable phenomenon) disappear; the material behavior becomes trivial. This conclusion has been reached independently by several researchers who have approached the subject from very different perspectives [2, 9, 13, 31, 57, 77, 89, 93, 107]. In [98], we developed[6] a non-asymptotic homogenization theory for periodic electromagnetic structures; the procedure is summarized in Section D below.

V Homogenization and Symmetry Breaking

A The Problem

The breakdown of asymptotic (zero-cell-size-limit) homogenization manifests itself, in particular, in the case of *incompatible symmetries* between the scattering characteristics of the original heterostructure and the respective homogenized sample. As an example, consider wave propagation in a dielectric multilayer consisting of repeated layers labeled α and β, surrounded by air, as shown in Fig. 1(a). The layers have unequal dielectric constants ϵ_α and ϵ_β (which may be complex and dependent on the frequency ω), so that the heterostructure lacks mirror symmetry with respect to the normal direction n. In Fig. 1(b), the solid lines show the phases of the reflection coefficients $\mathcal{R}_{\alpha\beta}$ and $\mathcal{R}_{\beta\alpha}$, calculated analytically using the transfer matrix technique [106], for s-polarized waves impinging normally on the structure with $\alpha\beta\ldots$ and $\beta\alpha\ldots$ layer orderings, respectively. (Reflection coefficients are the ratios of the complex amplitudes of the electric field in the reflected and incident waves.) In the static limit $a/\lambda \to 0$, the order of the layers is unimportant, but for larger values of a/λ the phases differ substantially [2, 31, 54, 107]. We call this effect, which arises

[6] This is joint work with Vadim Markel.

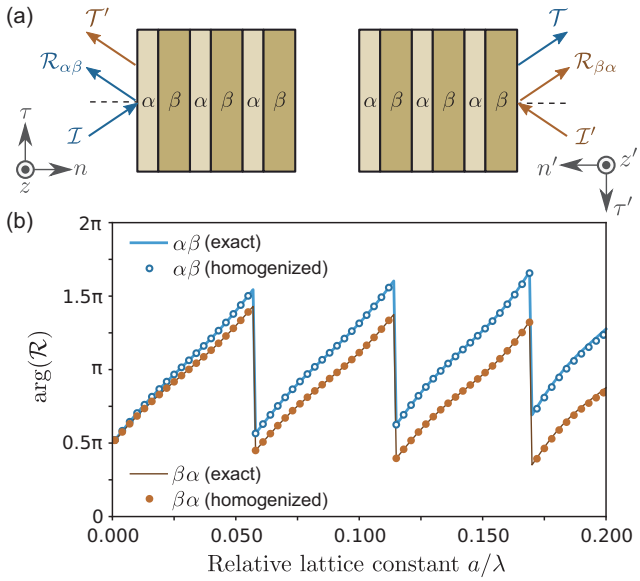


Figure 1: [From [97], by permission.] (a) Schematic of a multilayer heterostructure consisting of two layers a and b repeated an integer number of times. The layers have dielectric constants ϵ_α and ϵ_β, and are surrounded by air ($\epsilon = 1$). (b) Phases of the two reflection coefficients $R_{\alpha\beta}$ and $R_{\beta\alpha}$ versus relative lattice constant a/λ, where λ is the free space wavelength. The multilayer has $\epsilon_\alpha = 1$, $\epsilon_\beta = 5$, equal layer widths $d_\alpha = d_\beta = a/2$, with a total of 5 lattice periods (10 layers). The incident plane waves are s polarized (**E** parallel to z and **H** lying in the n-τ plane). Solid lines: exact values calculated via the transfer matrix technique; markers: results for the the homogenization method described in the text.

from the lack of mirror symmetry of the underlying heterostructure, *intrinsic symmetry breaking* (ISB).

A related but different effect, which we call *extrinsic symmetry breaking* (ESB), manifests itself when the external media on the two sides of the structure are different. In that case, not only the phases but also the magnitudes of the reflection coefficients may differ [31]. When the medium on one side is optically denser than the static average in the slab, different layer orderings can produce extremely different reflection coefficients when the incident wave is close to the critical angle for total internal reflection. (This phenomenon does not contradict optical reciprocity [79].)

At first glance, it seems that ISB cannot be faithfully reproduced by a homogenized slab, since a homogenous medium would have an inherent mirror symmetry ensuring that $\mathcal{R}_{\alpha\beta} = \mathcal{R}_{\beta\alpha}$.

To rectify that, Lei *et al.* introduced an artificial matched layer on the illumination side [54]. However, this is not satisfactory, since an effective medium ought to reflect the intrinsic characteristics of the structure, independent of the illumination conditions. In particular, if the layered slab is illuminated from both sides, then *two* artificial layers would have to be introduced, and their matching properties would be frustrated due to the coupling between those layers.

In contrast, we have shown [97] that an appropriate homogenization scheme can accurately account for ISB via magnetoelectric (ME) couplings in the effective material tensor. No artificial matching layers, auxiliary boundary conditions or complicated nonlocal formulations are required. Details about the homogenization scheme are given below; when applied to the above multilayer structure, it produces the values plotted as markers in Fig. 1(b), which

are in excellent agreement with the exact transfer matrix results. In particular, $\arg(\mathcal{R}_{\alpha\beta}) = \arg(\mathcal{R}_{\beta\alpha})$ in the $a/\lambda \to 0$ limit, but these values differ for shorter wavelengths, so that ISB is quantitatively accounted for.

B Magnetoelectric Coupling

In their most general form, local linear constitutive relations couple one pair of electric and magnetic fields to the other pair. For example, the $\mathbf{D}, \mathbf{H}$ fields could be expressed as linear combinations of $\mathbf{E}$ and $\mathbf{B}$ [4, 52, 53]. Equivalently, by a linear transformation, one can write the $\mathbf{E}$, $\mathbf{H}$ pair in terms of $\mathbf{D}$, $\mathbf{B}$ (e.g. [48]) or, alternatively, $\mathbf{D}$, $\mathbf{B}$ via $\mathbf{E}$, $\mathbf{H}$ [50, 65]. We do not investigate the most general bi-anisotropic relations, with their related controversies (non-reciprocity, the Post constraint) [48, 52, 53] but focus, as a case study, on s-waves propagating through a material slab (although p-polarization could be handled in a similar way). The 3-vector (D, B_n, B_τ) gets expressed via the 3-vector (E, H_n, H_τ); in general, this relationship couples electric and magnetic fields, as discussed below.

C Magnetoelectric Coupling for s-Polarization

To elucidate the origin of ME coupling, we first consider the simple case of an isotropic lossless homogeneous medium with two s-polarized plane waves propagating in opposite axial directions $\pm n$, indicated in Fig. 1(a). The respective equal-magnitude wave vectors are $\pm\mathbf{q} = \pm q\,\hat{\mathbf{q}}$, where q is the wavenumber in the medium and $\hat{\mathbf{q}}$ is a unit vector; the respective electric and magnetic field components are

$$E_z^{\pm} = E_0^{\pm} \exp(\pm iq\,\hat{\mathbf{q}}\cdot\mathbf{r}), \quad H_\tau^{\pm} = H_0^{\pm} \exp(\pm iq\hat{\mathbf{q}}\cdot\mathbf{r}), \quad (10)$$

where $\mathbf{r} = (n, \tau, z)$. The waves satisfy Maxwell's equations

$$\nabla\times\mathbf{E} = ik_0\mathbf{B}; \quad \nabla\times\mathbf{H} = -ik_0\mathbf{D} \quad (11)$$

under the $\exp(-i\omega t)$ phasor convention. The medium is described by a material tensor $\mathcal{M}$ whose matrix representation M in a given coordinate system satisfies

$$\Psi_{DB} = M\,\Psi_{EH} \quad (12)$$

$$\Psi_{DB} = \begin{bmatrix} D_{0z}^{+} & D_{0z}^{-} \\ B_{0\tau}^{+} & B_{0\tau}^{-} \end{bmatrix}, \quad \Psi_{EH} = \begin{bmatrix} E_{0z}^{+} & E_{0z}^{-} \\ H_{0\tau}^{+} & H_{0\tau}^{-} \end{bmatrix}. \quad (13)$$

Normalizing the $E_{0z}^{\pm}$ amplitudes to unity and applying Maxwell's equations gives

$$\Psi_{DB} = q\begin{bmatrix} -Y_+ & Y_- \\ -1 & 1 \end{bmatrix}, \quad \Psi_{EH} = \begin{bmatrix} 1 & 1 \\ Y_+ & Y_- \end{bmatrix}, \quad (14)$$

where $Y_\pm = H_{0\tau}^{\pm}/E_{0z}^{\pm}$ are the wave admittances. Then

$$M = \Psi_{EH}^{-1}\Psi_{DB} = \frac{q}{Y_2 - Y_1}\begin{bmatrix} -2Y_1Y_2 & Y_1+Y_2 \\ -(Y_1+Y_2) & 2 \end{bmatrix} \quad (15)$$

$$\begin{bmatrix} D_z \\ B_\tau \end{bmatrix} = M \begin{bmatrix} E_z \\ H_\tau \end{bmatrix} \quad (16)$$

The ME coupling is represented by the off-diagonal terms in M, and is absent if and only if $Y_1 = -Y_2$, which is the case for an ordinary homogeneous dielectric medium.

In a periodic medium, the two plane waves (10) are replaced with Bloch waves, and $Y_{1,2}$ are the boundary admittances of these Bloch waves. We conclude from (15) that *ME coupling arises whenever these boundary admittances are different*, which in general is indeed the case for non-symmetric structures.

Note that this type of ME coupling is not equivalent to optical activity. It does not alter the polarization of the wave, which remains s-polarized throughout. By contrast, the constitutive relations for optically active media typically include a contribution to $\mathbf{D}$ in the direction of $\mathbf{B}$, as well as a contribution to $\mathbf{B}$ in the direction of $\mathbf{E}$ [4, 8, 23].

D Homogenization Procedure

We now adopt the homogenization scheme described in [94, 98], which generates an effective tensor $\mathcal{M}$ for a layered heterostructure by approximating the fields on two scales, one finer and the other one coarser than the lattice cell size. The fine-scale fields are approximated by a basis set of Bloch waves traveling in different directions. The coarse-scale basis consists of the respective generalized plane waves, which must satisfy (i) Maxwell's equations within the sample and (ii) Maxwell's boundary conditions for the tangential components of the electric and magnetic fields on the boundary of the sample.

To satisfy (ii), the plane wave amplitudes are computed as boundary averages of the periodic factors of Bloch waves; to satisfy (i), the M matrix is found by solving a linear algebra problem analogous to (12), except that now the Ψ_{DB} and Ψ_{EH} matrices are rectangular, with the number of columns equal to the number of basis functions. Hence (12) is in general interpreted in the least squares sense rather than as an exact equality; see [94, 98] for further details.

E Intrinsic Symmetry Breaking: Analytical Insight

We apply this procedure to s-polarized waves in the multilayer heterostructure of Fig. 1(a) (the p-wave case can be dealt with similarly). To get an analytical insight, we again take all the materials to be lossless, so that ϵ_α and ϵ_β are real, and consider a fine-scale basis of only two Bloch waves propagating in the normal direction n, with their Bloch wave-numbers $\pm q$ at the operating frequency:

$$e_1(n) = u(n)\exp(iqn) \quad (17)$$

$$h_{1\tau}(n) = -k_0^{-1}[qu(n) - iu'(n)]\exp(iqn) \quad (18)$$

$$e_2(n) = u^*(n)\exp(-iqn) \quad (19)$$

$$h_{2\tau}(n) = k_0^{-1}[qu^*(n) + iu^{*\prime}(n)]\exp(-iqn). \quad (20)$$

Here $u(n)$ denotes the lattice-periodic factor for the electric field, and '*' indicates complex conjugates. On the coarse scale, our procedure defines the EH-amplitudes of plane waves as the *boundary values* ($n = 0$) of the Bloch waves:

$$E_{0z}^{+} = u(0), \qquad H_{0\tau}^{+} = -k_0^{-1}[qE_0^{+} - iu'(0)], \quad (21)$$

$$E_{0z}^{-} = u^*(0), \qquad H_{0\tau}^{-} = \;\; k_0^{-1}[qE_0^{-} + iu^{*\prime}(0)]. \quad (22)$$

The corresponding admittances are therefore

$$Y_1 = -k_0^{-1}\left[q - i\tilde{e}_1'(0)/\tilde{e}_1(0)\right] \quad (23)$$

$$Y_2 = \;\; k_0^{-1}\left[q + i\tilde{e}_1^{*\prime}(0)/\tilde{e}_1^{*}(0)\right]. \quad (24)$$

An explicit expression for the ME coupling term is

$$M_{12} = i\,\frac{q}{k_0}\,\frac{\mathrm{Re}\,\eta}{\mathrm{Im}\,\eta + q}, \qquad \eta \equiv \frac{u'(0)}{u(0)}. \quad (25)$$

Hence the ME coupling arises from the difference in the boundary admittances of the Bloch waves. If the lattice

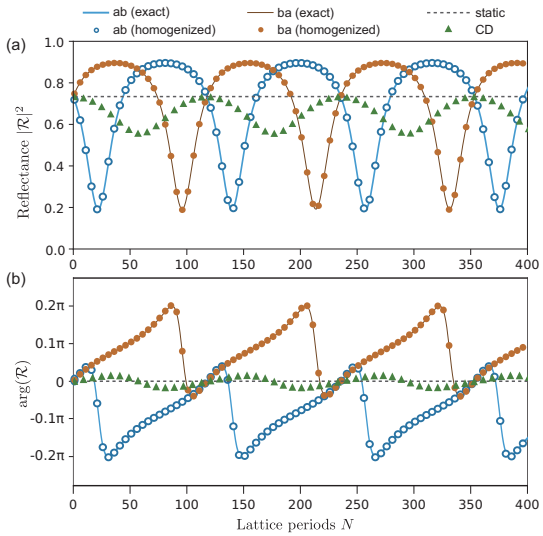


Figure 2: [From [97], by permission.] Scattering characteristics of a multilayer with asymmetric external media. The structure consists of N identical cells, each containing two layers, 'α' and 'β', with the thicknesses $d_\alpha = d_\beta = 10$ nm and dielectric constants $\epsilon_\alpha = 5$ and $\epsilon_\beta = 1$. Free-space wavelength $\lambda = 500$ nm (i.e. $a/\lambda = 0.04$). External dielectric constants are $\epsilon_{\text{in}} = 4$ and $\epsilon_{\text{out}} = 3$ on the sides of incidence and transmission, respectively. (These parameters match the ones of [31].) Incidence is at the critical angle (26). (a) reflectances $|\mathcal{R}_{\alpha\beta}|^2$ and $|\mathcal{R}_{\beta\alpha}|^2$; (b) reflection coefficient phases $\arg(\mathcal{R}_{\alpha\beta})$ and $\arg(\mathcal{R}_{\beta\alpha})$ vs. N. Solid curves: exact values calculated via the transfer matrix method. Markers: results for homogenization with magnetoelectric coupling [94, 98]. Two layer orderings, $\alpha\beta\ldots$ and $\beta\alpha\ldots$, exhibit significantly different behaviors. Static homogenization (horizontal dashed lines) and "current-driven" homogenization (CD, green triangles) yield qualitatively inaccurate results.

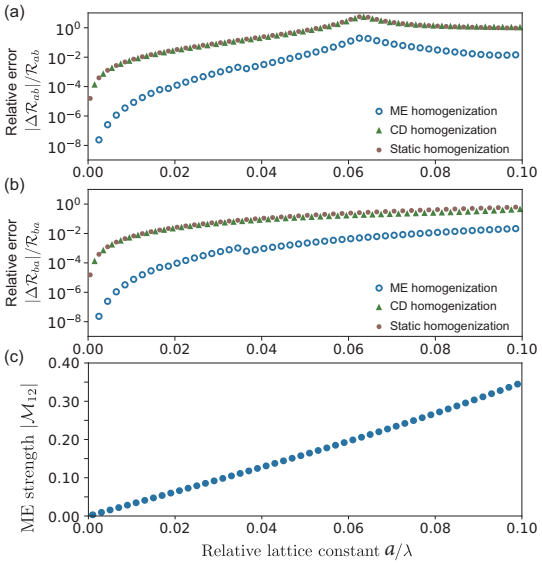


Figure 3: [From [97], by permission.] Relative errors and effective ME coupling strengths versus normalized lattice constant a/λ, with all other parameters the same as in Fig. 2; structure with 10 lattice cells. (a, b) Relative errors in $\mathcal{R}_{\alpha\beta}$ and $\mathcal{R}_{\beta\alpha}$, respectively, calculated using the static, "current-driven" (CD) and ME homogenization as compared to the transfer matrix results. Note the logarithmic scale on the vertical axis. (c) Magnitude of the off-diagonal element in the effective M matrix, which describes the strength of the ME coupling.

cell possesses mirror symmetry, then the derivative $u'(0)$ vanishes, so $M_{12} = 0$.

Importantly, the matrix representation of $\mathcal{M}$ depends on the choice of coordinate system. If (n, τ, z) is switched to the mirror-image system (n', τ', z) shown in Fig. 1(a), the off-diagonal ME terms reverse sign. The effective medium is thus able to capture the effects of the broken mirror symmetry, as demonstrated by the numerical results of Fig. 1(b).

F Example: Local Homogenization and Extrinsic Symmetry Breaking

Turning now to ESB effects, we set the same parameters as in [31]: equal layer widths $d_\alpha = d_\beta = a/2 = 10$ nm, dielectric constants $\epsilon_\alpha = 5$ and $\epsilon_\beta = 1$, and free-space wavelength $\lambda = 500\,\text{nm}$. The effective permittivity for the s mode in the static limit ($a/\lambda \to 0$) is $\epsilon_{\text{stat}} = (\epsilon_\alpha d_\alpha + \epsilon_\beta d_\beta)/a = 3$. The number of lattice cells N is allowed to vary. External dielectric permittivities are $\epsilon_{\text{in}} = 4$ and $\epsilon_{\text{out}} = 3$ on the sides of incidence and transmission, respectively. These parameters match the ones of [31] and, since $\epsilon_{\text{in}} \neq \epsilon_{\text{out}}$, give rise to ESB. In the static limit, the critical angle for total internal reflection is

$$\theta_{\text{crit}} = \sin^{-1}\sqrt{\epsilon_{\text{stat}}/\epsilon_{\text{in}}} = 60^\circ. \tag{26}$$

Once the angle of incidence reaches the critical value, the wave in the β layer becomes evanescent, but the wave in the α layer is propagating.

For this setup, the fine-scale basis in our homogenization procedure contains Bloch waves with the tangential components of the Bloch wave vector $q_{\tau m} = m\epsilon_{\text{stat}}^{\frac{1}{2}}k_0/(m_q - 1)$, where $0 \le m < m_q$, and m_q is a parameter defined below. Only non-negative values of q_τ are needed due to the symmetry of the structure in the tangential direction. For each q_τ there are two Bloch waves in the forward and backward directions; hence the total size of the Bloch basis is $2m_q$. On the coarse level, the basis consists of the respective $2m_q$ generalized plane waves. We will take $m_q = 7$; the results are essentially unchanged for other choices of $m_q \ge 5$.

Near θ_{crit}, the reflection and transmission coefficients are found to depend strongly on the choice of layer order ($\alpha\beta\ldots$ or $\beta\alpha\ldots$), and both are very different from the value predicted by the static permittivity ϵ_{stat}; see [31] and Fig. 2. Plots in Fig. 2 show the reflectance and the phase of the reflection coefficient against the number of lattice periods N in the slab. (Since each until cell has two layers, the total number of layers is $2N$.) To our knowledge, no published homogenization procedures are capable of accurately reproducing transmission and reflection from asymmetric structures, unless an auxiliary artificial layer is introduced, as done by Lei *et al.* [54]. (As already noted, such a layer does not represent intrinsic characteristics of the structure and is good for one-sided illumination only.)

In Fig. 2 we compare our homogenization results with both classical quasi-static (QS) homogenization and the popular "current-driven" (CD) homogenization scheme [86] without artificial matching layers. (Implementation of CD homogenization is described in detail in [61].)

It is clear that the QS and CD results are qualitatively inaccurate in this case. This is not surprising because, among other things, QS and CD models do not include a mechanism for representing ISB; in particular, $R_{CD} = R_{CD,\alpha\beta} = R_{CD,\beta\alpha}$ unless artificial boundary layers are introduced.

In contrast, our homogenization produces magnetoelectric coupling automatically and yields TR coefficients agreeing extremely well with the exact results obtained by

transfer matrix calculations (Fig. 2). More specifically, Figs. 3(a,b) show that the relative errors in the reflection coefficients $\mathcal{R}_{\alpha\beta}$, $\mathcal{R}_{\beta\alpha}$ are at least two orders of magnitude lower than in static or CD homogenization.

Our homogenization captures the substantial differences between the $\alpha\beta\ldots$ and $\beta\alpha\ldots$ layer orderings [31] via the ME coupling in the $\mathcal{M}$ tensor. For instance,

$$M(a/\lambda = 0.04) \approx \begin{bmatrix} 3.02 & 0 & -0.128i \\ 0 & 1 & 0 \\ 0.128i & 0 & 1 \end{bmatrix}. \qquad (27)$$

or more explicitly $D_z \approx 3.02E_z - 0.128iH_\tau$; $B_n \approx H_n$; $B_\tau \approx 0.128iE_z + H_\tau$. The effective permittivity differs slightly from its static value of 3, but the key feature is the presence of the ME coupling terms, which are clearly appreciable. The magnitude of the ME coupling is approximately proportional to a/λ and vanishes in the static limit $a/\lambda \to 0$, as shown in Fig. 3(c).

G Conclusion

We have demonstrated that our homogenization procedure [94,98], which automatically produces an effective material tensor with magnetoelectric coupling terms, can accurately describe the behavior of periodic multilayer heterostructures away from the static limit. The general features of this procedure are as follows:

1. The effective material tensor is independent of the illumination conditions.
2. The effective tensor automatically accounts for anisotropy, magnetic response and magnetoelectric coupling.
3. Intrinsic and extrinsic symmetry breaking are rendered accurately. No artificial boundary layers, nonlocal effects or other amendments are employed.

In contrast, to the best of our knowledge, in the existing publications the only way to account for ISB is via an artificial matching layer introduced on the boundary of the sample. Such a layer is extrinsic to the sample and works only for one-sided illumination. If a layered slab is illuminated from both sides, then two artificial layers would need to be introduced; however, the coupling between them will debilitate the matching (not to mention possible extensions of the theory to 2D and 3D samples finite in all coordinate directions).

Any local homogenization will break down once the wavelength becomes sufficiently short. The accuracy of our procedure at short wavelengths was examined in prior publications [94,98]; this accuracy is significantly improved in the nonlocal version of our method [94].

VI One Layer is "Bulk"

A General Considerations

In existing effective medium theories of periodic electromagnetic structures, it is commonly assumed that bulk behavior emerges only if the number of layers in a given structure is sufficiently large. For example, in [91] the effective medium representation of a certain family of hyperbolic metamaterials was determined to be accurate, typically, for five or more layers in the sample, although the results do vary depending on the composition of the structure. In [58], the authors studied particular metamaterial absorbers and found that four layers could already be accurately characterized as an effective medium. In other publications, as little as three layers were deemed sufficient [14,78]. Theoretical analysis of convergence to bulk behavior has in general been perceived as quite involved due to the complexity of surface waves [60,105].

The thickness of the sample is commonly believed to affect the accuracy of homogenization in two different ways. The first factor is the optical length (OL), defined as the phase shift of the wave propagating across the sample (a Bloch wave in a periodic structure or a plane wave in a homogeneous medium). For a large OL, minor deviations in the wavenumber may strongly affect the predicted transmission coefficient (especially its phase) as well as reflection. The second factor, as noted above, is the putative convergence to bulk characteristics (CB), once the thickness of the sample (the number of layers) has approached or crossed a certain threshold.

While the OL influence in real, we have shown, through theoretical analysis and numerical examples, that CB is a non-issue; in a sense, one layer is already bulk.

Consider a slab with N layers, thickness $d = Na$ in the normal (n) direction and infinite in the tangential directions τ, z, (n, τ, z) being a right-handed system. The slab is illuminated by a plane wave propagating from the air ($n < 0$) in the positive n direction. The slab/air interface is at $n = 0$.

For algebraic simplicity, let us assume translational invariance in the z direction and the s mode – one-component electric field $\mathbf{e}(\mathbf{r}) = \hat{z}\, e(\mathbf{r})$ and the respective two-component magnetic field $\mathbf{h}(\mathbf{r}) = \hat{n}h_n(\mathbf{r}) + \hat{\tau}h_\tau(\mathbf{r})$, where $\mathbf{r} \equiv (n, \tau)$. The analysis is extendable to the general 3D case.

For a given q_τ, consider a superposition of the forward and backward Bloch waves:

$$e(\mathbf{r}) = [c_1\tilde{e}_1(n,\tau)\exp(iq_{n1}n) + c_2\tilde{e}_2(n,\tau)\exp(iq_{n2}n)]\exp(iq_\tau\tau) \qquad (28a)$$

$$h_\tau(\mathbf{r}) = \left[c_1\tilde{h}_{\tau1}(n,\tau)\exp(iq_{n1}n) + c_2\tilde{h}_{\tau2}(n,\tau)\exp(iq_{n2}n)\right]\exp(iq_\tau\tau) \qquad (28b)$$

where $c_{1,2}$ are undetermined coefficients and $q_{n1} = -q_{n2}$ are the normal components of the respective Bloch wave vectors.

Let $\mathbf{s}(n,\tau)$ be any vector field of the form

$$\mathbf{s}(n,\tau) = \tilde{\mathbf{s}}(n)\exp(ik_\tau\tau) \qquad (29)$$

over any lattice cell face $\mathbb{F}$ parallel to the τz-plane. We will need the following operator, averaging the tangential component of $\mathbf{s}$ on $\mathbb{F}$:

$$\mathcal{A}\,\mathbf{s}(n) \equiv a^{-2}\int_{\mathbb{F}} \mathbf{n}\times\mathbf{s}(n,\tau)\,\exp(-ik_\tau\tau)\,d\mathbb{F} = a^{-2}\int_{\mathbb{F}} \mathbf{n}\times\tilde{\mathbf{s}}(n,\tau)\,d\mathbb{F} \qquad (30)$$

where the coordinate n corresponds to the location of $\mathbb{F}$ and $\mathbf{n}$ is the unit normal vector in the positive n direction. Although the $\mathcal{A}$ operator depends on $\mathbb{F}$ and hence on n,

with a slight abuse of notation we write $\mathcal{A}\mathbf{s}(n)$ instead of $\mathcal{A}(n)\mathbf{s}(n)$.

Consider now an arbitrary lattice cell – for convenience, $0 \le n, \tau \le a$, although the relations below will apply to any cell. The amplitudes $c_{1,2}$ of (28a), (28b) are linearly related to the averages of (e, h_τ) on the left boundary of the cell:

$$\begin{bmatrix} c_1 \\ c_2 \end{bmatrix} = Z(0)^{-1} \begin{bmatrix} \mathcal{A}\, e(0) \\ \mathcal{A}\, h_\tau(0) \end{bmatrix}, \tag{31a}$$

$$Z(0) \stackrel{\text{def}}{=} \begin{bmatrix} \mathcal{A}\, e_1(0) & \mathcal{A}\, e_2(0) \\ \mathcal{A}\, h_{\tau 1}(0) & \mathcal{A}\, h_{\tau 2}(0) \end{bmatrix} \tag{31b}$$

Since Bloch waves are defined up to an arbitrary factor, it is convenient to rescale the second row of $Z(0)$ to unity and redefine $Z(0)$ as

$$Z(0) = \begin{bmatrix} z_1 & z_2 \\ 1 & 1 \end{bmatrix} \tag{32}$$

where z_1, z_2 are Bloch impedances whose definition is clear from the context and is consistent with the one in [87,88].

Keeping this in mind, we can proceed with the standard transfer matrix analysis [106], except that Bloch waves rather than plane waves are involved. The total face-averaged field at the boundary $n = a$ is

$$\begin{aligned} \begin{bmatrix} \mathcal{A}\, e(a) \\ \mathcal{A}\, h_\tau(a) \end{bmatrix} &= \begin{bmatrix} \mathcal{A}\, e_1(a) & \mathcal{A}\, e_2(a) \\ \mathcal{A}\, h_{\tau 1}(a) & \mathcal{A}\, h_{\tau 2}(a) \end{bmatrix} \begin{bmatrix} c_1 \\ c_2 \end{bmatrix} \\ &= \begin{bmatrix} \mathcal{A}\, e_1(0) & \mathcal{A}\, e_2(0) \\ \mathcal{A}\, h_{\tau 1}(0) & \mathcal{A}\, h_{\tau 2}(0) \end{bmatrix} Q \begin{bmatrix} c_1 \\ c_2 \end{bmatrix} \\ &\stackrel{(31a)}{=} Z(0)\, Q\, Z(0)^{-1} \begin{bmatrix} \mathcal{A}\, e(0) \\ \mathcal{A}\, h_\tau(0) \end{bmatrix} \equiv T_{\mathbb{C}} \begin{bmatrix} \mathcal{A}\, e(0) \\ \mathcal{A}\, h_\tau(0) \end{bmatrix} \end{aligned} \tag{33}$$

where

$$Q = \begin{bmatrix} \exp(iq_{n1}a) & 0 \\ 0 & \exp(iq_{n2}a) \end{bmatrix} \tag{34}$$

$$T_{\mathbb{C}} = Z(0)\, Q\, Z(0)^{-1} \tag{35}$$

For an N-layer slab, let us define

$$T_N \stackrel{\text{def}}{=} T_{\mathbb{C}}^{-N} = Z(0)\, Q^{-N} Z(0)^{-1} \tag{36}$$

Then the input-output relation for the slab is

$$\begin{bmatrix} E(0) \\ H_\tau(0) \end{bmatrix} = T_N \begin{bmatrix} E(Na) \\ H_\tau(Na) \end{bmatrix} \tag{37}$$

where

$$E(0) \stackrel{\text{def}}{=} \mathcal{A}e(0), \quad E(Na) \stackrel{\text{def}}{=} \mathcal{A}e(Na) \tag{38a}$$

$$H_\tau(0) \stackrel{\text{def}}{=} \mathcal{A}h_\tau(0), \quad H_\tau(Na) \stackrel{\text{def}}{=} \mathcal{A}h_\tau(Na) \tag{38b}$$

Expressing $E(Na)$, $H_\tau(Na)$ via the amplitude of the transmitted field E_t, we have

$$\begin{bmatrix} E(0) \\ H_\tau(0) \end{bmatrix} = T_N \Psi_{\text{out}} E_t, \quad \Psi_{\text{out}} \stackrel{\text{def}}{=} \begin{bmatrix} 1 \\ z_{\text{out}}^{-1} \cos\theta_{\text{out}} \end{bmatrix} \tag{39}$$

where z_{out} is the intrinsic impedance of the medium on the transmission side. Finally, writing $E(0), H_\tau(0)$ in terms of the amplitudes of the incident and reflected waves E_i, E_r, one obtains

$$\begin{bmatrix} E_i \\ E_r \end{bmatrix} = \Psi_{\text{in}}^{-1} T_N \Psi_{\text{out}} E_t \tag{40a}$$

$$\Psi_{\text{in}} \stackrel{\text{def}}{=} \begin{bmatrix} 1 & 1 \\ z_{\text{in}}^{-1} \cos\theta_{\text{in}} & -z_{\text{in}}^{-1} \cos\theta_{\text{in}} \end{bmatrix} \tag{40b}$$

where z_{in} is the intrinsic impedance of the medium on the side of incidence.

Although the algebra above may look cumbersome at first glance, it represents the standard layer-by-layer transfer matrix method applied to Bloch wave averages.

Due to (38), the differences between E and e, and between H and h on both sides of the slab (physically, these differences represent surface waves [60,105]) do not contain the zero-order harmonic with respect to τ and hence do not affect the far fields, as long as $a < \lambda_{\text{out}}$. This brings us to the following key

Proposition 1 *At any given angle of incidence, reflection and transmission coefficients are identical for any structures with the same values of the Bloch wavenumbers and impedances, regardless of the number of layers.*

Indeed, since matrices $Z(0)$ and Q depend only on the Bloch parameters, the same is true for the cell transfer matrix $T_{\mathbb{C}}$ (35) and hence for the relationship between the incident/reflected/transmitted fields (40a).

Furthermore, Proposition 1, along with (40a), leads to a natural definition of homogenization. Since effective material parameters must be intrinsic to the structure and independent of the outside media, and since the only such intrinsic term in (40a) is the transfer matrix T_N (36), the goal of homogenization must be to approximate this matrix as accurately as possible with an analogous matrix corresponding to a hypothetical homogeneous medium; that is, to minimize, with respect to a desired norm, the matrix difference

$$\begin{aligned} \Delta T \stackrel{\text{def}}{=} T_N - T_{Nh} \;=\; & Z(0)\, Q^{-N} Z(0)^{-1} \\ & - Z_h(0)\, Q_h^{-N} Z_h(0)^{-1} \end{aligned} \tag{41}$$

where the subscript 'h' indicates the respective matrix for a homogeneous layer with given parameters.

T_N involves four variables – the Bloch impedances z_1, z_2 and wavenumbers q_{n1}, q_{n2} – which are functions of the angle of incidence. If the effective parameters are also allowed to depend on the angle, as done in some existing theories (e.g. [13, 16]), then matrices $Z_h(0)$, Q_h may be angle-dependent as well. Under these assumptions, perfect homogenization is possible, since the material tensor has 9 adjustable entries, allowing an ideal fit for the four parameters of T_N. Hence we arrive at the following known result:

Proposition 2 *If the effective parameters are allowed to depend on the angle of incidence, then homogenization can be perfect irrespective of the number of layers.*

On the other hand, for an effective tensor *independent of illumination conditions* [61,98], error ΔT (41) is in general nonzero. For small deviations $\delta z_{1,2} = z_{1,2h} - z_{1,2}$, $\delta q_{1,2} = q_{1,2h} - q_{1,2}$, perturbation analysis gives the Frobenius norm

$$\|\Delta T\|_F \;=\; \mathcal{O}(\delta z_{1,2},\; N\delta q_{1,2}) \tag{42}$$

The N factor is a clear manifestation of the OL effect. At the same time, there is no indication of the putative CB phenomenon.

While the s mode was considered to fix ideas, the analysis and results can be extended to arbitrary structures with arbitrary excitation, even for polarization rotation. The only

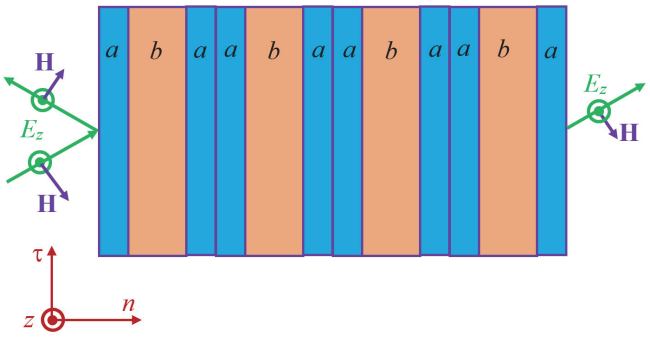


Figure 4: [From [37], by permission.] The setup for the example of a layered structure. The lattice cell contains three layers, *aba*, with their respective widths w_a, w_b, w_a and dielectric permittivities ϵ_a, ϵ_b, ϵ_a. Oblique incidence, *s*-polarization ($E = E_z$, **H** in the $n\tau$ plane).

stipulation in this general case is existence, for a given angle of incidence, of four linearly independent Bloch waves[7] (backward/forward, with two different polarizations). The Z, $T_{\mathbb{C}}$ and T_N matrices are in general 4×4 and act on the 4-vectors $(E_{\tau 1}, E_{\tau 2}, H_{\tau 1}, H_{\tau 2})$.

B Numerical Example: Layered Media

Under plane wave illumination, fields in periodic layered media (with a finite thickness $d = Na$ in the normal n direction, and infinite in the τz directions) are mathemtatically described by ordinary differential equations with respect to n and therefore are linear combinations of two linearly independent solutions, which can conveniently be chosen as Bloch waves. Consequently, there are no surface waves ("transition layers"), and it follows from the analysis above that the retrieved effective material parameters must be completely independent of the number of layers.

As a numerical example, we consider a benchmark problem established in previous publications [61, 94, 98], Fig. 4. The lattice cell has mirror symmetry and contains three dielectric layers (a, b, a), with their respective permittivities $\epsilon_a, \epsilon_b, \epsilon_a$ and widths $(1/4, 1/2, 1/4)\, a$. The materials are intrinsically nonmagnetic. Free space is assumed on the sides of illumination and transmission; *s*-polarization is considered ($E = E_z$, **H** is in the $n\tau$ plane, with different directions and magnitudes for the incident, reflected and transmitted waves).

For a numerical investigation, we have adopted straightforward parameter retrieval, to avoid any real or perceived idiosyncrasies of any other homogenization procedures. Finding the material tensor from the transmission and reflection data at normal incidence only is well known to be an underdetermined problem [61, 90]. This is related mathematically to the multivaluedness of the inverse trigonometric functions, and physically to a varying number of wavelengths within a homogenized slab with a high undetermined optical density. Retrieval becomes well-posed if, in addition to normal incidence, other angles are taken into account. A semi-analytical procedure for parameter retrieval at angles *around* normal incidence is detailed in [61].

As a simple alternative, here we apply numerical optimization for the following set of angles of incidence:

$$\underline{\theta} = \{0, \pm 5^\circ, \pm 10^\circ, \pm 45^\circ\} \tag{43}$$

[7] Linear independence is stipulated here only for the *boundary values* of the respective Bloch waves.

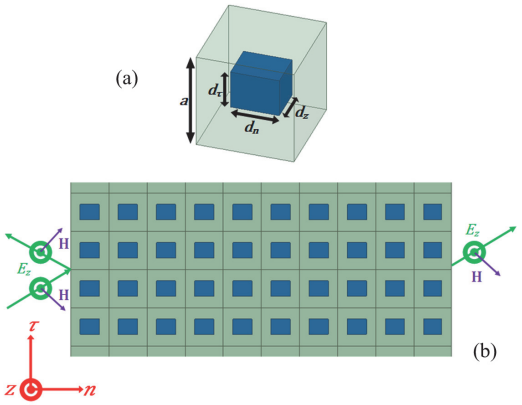


Figure 5: [From [37], by permission.] (a) The unit cell for the 3-D example: a rectangular silver cuboid ($d_n \times d_\tau \times d_z$) in a host material with the permittivity 1.0; $d_n = 100$ nm, $d_\tau = d_z = 80$ nm. The cell size is $a_x = a_y = a_z = a = 200$ nm. (b) Top view of the sample structure (truncated in $\pm\tau$ direction); illumination by an *s*-polarized plane wave from the left; z-periodicity.

The objective function is

$$G(\mathcal{M}, \underline{\theta}, N) = \|\underline{R}_h - \underline{R}_{\text{layered}}\|_2 + \|\underline{T}_h - \underline{T}_{\text{layered}}\|_2 \tag{44}$$

Here $\underline{R}_h$, $\underline{R}_{\text{layered}}$, $\underline{T}_h$, $\underline{T}_{\text{layered}}$ are the Euclidean vectors of the complex reflection and transmission coefficients, respectively, corresponding to a given set of incidence angles $\underline{\theta}$; subscripts 'h' and 'layered' correspond to the homogenized slab with a material tensor $\mathcal{M}$ and to the actual layered structure, respectively. Similar notation is used for the sets of transmission coefficients. Minimization of the functional G (44) was performed numerically using Matlab's built-in function `fminsearch`, with the tolerance of 10^{-6}. The number of layers N varied from 1 through 10. For $a/\lambda = 0.2$ (i.e. the vacuum wavelength equal to five cell sizes), and for $\epsilon_a = 4 + 0.1i$, $\epsilon_b = 1$ the effective parameters are found to be $\epsilon_{\text{eff}} = 2.0397 + 0.0165i$, $\mu_{nn,\text{eff}} = 1.2347 + 0.0826i$, $\mu_{\tau\tau,\text{eff}} = 1.2883 + 0.0163i$. These results are entirely independent of the number of layers.

C Numerical Example: A 3D plasmonic structure

Our second example is more involved: a rectangular silver parallelepiped $d_n \times d_\tau \times d_z$ at the center of an otherwise empty lattice cell $a \times a \times a$ (Fig. 5). Illumination is by an *s*-polarized plane wave. Due to symmetry, the effective material tensor is diagonal. Particular geometric parameters chosen for this example are $d_n = 100$ nm, $d_\tau = d_z = 80$ nm, $a = 200$ nm.

We use the following form of the Drude model for silver:

$$\epsilon(\lambda) = \epsilon_0 - \frac{1}{\lambda_p^2/\lambda^2 + i\tilde{\gamma}\lambda_p/\lambda} \tag{45}$$

where $\lambda = 2\pi c/\omega$ is the free-space wavelength corresponding to a given frequency ω; $\epsilon_0 = 5$; $\tilde{\gamma} = 1/526.3$; $\lambda_p = 136.1$ nm [80].

For our full-wave 3D simulations, we have chosen the publicly available Rigorous Coupled Wave Analysis (RCWA) [63, 64] tool S^4 [56], which has been extensively used and tested by various research groups and in our prior publications [38, 39]. S^4 is freely available on the nanohub server [44].

RCWA splits up a 3D structure with 2D periodicity into thin slices. 2D Fourier expansions within each slice are

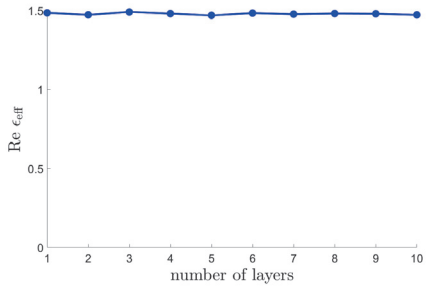


Figure 6: [From [37], by permission.] The real part of the retrieved ϵ_{eff} for the 3D plasmonic heterostructure vs. the number of layers. $\lambda = 1200$ nm, $a = 200$ nm, angles used for retrieval [deg.]: 0, 5, 10, 45. There is no indication of gradual "convergence to bulk".

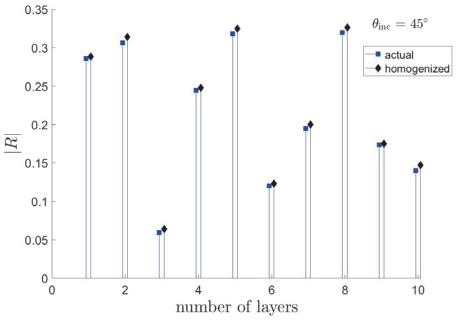


Figure 7: [From [37], by permission.] The absolute value of the reflection coefficient R vs. the number of layers, for the actual heterostructure and the respective homogeneous slab. $\lambda = 1200$ nm; the angle of incidence is 45° (numerical results for other angles lead to the same conclusions). The stems are displaced slightly relative to their integer positions for visual clarity.

matched across the interface boundaries between the slices to enforce the continuity of the tangential field components. In most our simulations, the number of in-plane Fourier coefficients is $N_s = 100$, but we have also verified consistency of the results in selected cases with $N_s = 400$. Transmission and reflection coefficients have been computed for structures with one to ten layers at the free-space wavelength $\lambda = 1200$ nm.

The parameter retrieval procedure and the objective function (44) are the same as in the previous example.

Plotted in Fig. 6 is the real part of the retrieved effective permittivity ϵ_{eff} for the 3D plasmonic heterostructure as a function of the number of layers. Results for the effective magnetic parameters $\mu_{n,\text{eff}}$ and $\mu_{\tau,\text{eff}}$ are qualitatively similar [37]; the imaginary parts of all these parameters are on the order of 0.01 and not shown. All parameters exhibit just minor deviations from a constant value, and, consistent with our analysis above, there is no evidence of a gradual transition to bulk values.

This conclusion can be reinforced by looking at the results in a slightly different way. Suppose that parameter retrieval is performed just for a single layer of the structure under consideration. By conventional wisdom, these parameters would not be applicable to the "bulk". However, the numerical results paint a different picture. Compared in Fig. 7 are the absolute values of the reflection coefficients for the actual heterostructure and the respective homogenized slab, as functions of the number of layers, for $\theta_{\text{inc}} = 45°$. The agreement between the two is evident for all numbers

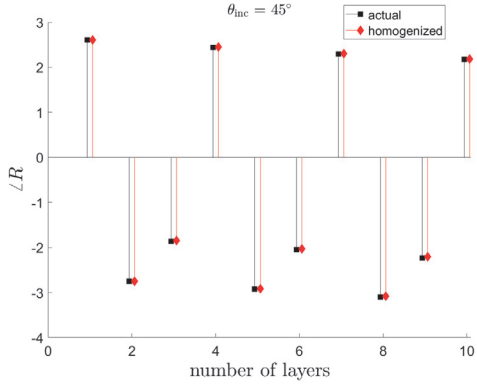


Figure 8: [From [37], by permission.] Same as in Fig. 7, but for the phase angle of R.

of layers, despite the fact that parameter retrieval was performed for a single layer only. (Numerical results for other angles of incidence lead to the same conclusion.) A similar agreement is manifest for the phase angle of R (Fig. 8) as well as for the magnitudes and phases of the transmission coefficients [37].

There is, however, an important caveat. In the case under consideration, effective parameters are virtually independent of the angle of incidence. This means that the heterostructure is homogenizable in the traditional sense. Then, as our theory and results show, effective parameters do not depend on the number of layers. On the other hand, if parameters are allowed to be illumination-dependent,[8] then homogenization can render reflection and transmission coefficients perfectly, and the effective (angle-dependent) parameters are, yet again, independent of the number of layers.

As noted in the introduction, parameters retrieved for a small number of layers were often recognized by various research groups to be physically meaningful [14, 58, 78, 91]; this is consistent with the primary message of this section. If a dependence of effective parameters on the number of layers is observed, it is likely due to a combination of factors: (i) numerical and/or measurement errors and fabrication tolerances, and (ii) structure not being homogenizable because of its complexity and/or wavelengths being short.

D Discussion and Conclusion

Homogenization is aimed at replacing a periodic heterostructure with a homogeneous sample of the same size and shape, in such a way that transmission and reflection (or, more generally, scattering) of the incident radiation remains unchanged or changes as little as possible. In the case of a homogeneous slab illuminated by a linearly polarized plane wave at any fixed angle of incidence, the field within the slab, under rather general assumptions, is a superposition of two independent plane waves – forward and backward. Notably, the same is true for the periodic structure, except that the superposition is of the forward and backward *Bloch waves* rather than plane waves.

This leads to the following correspondence principle, stated as Proposition 1 above. If the boundary impedance and wavenumber for a homogeneous layer are the same as those of the periodic structure, the scattering parameters

[8] Here we do not debate the usefulness of illumination-dependent parameters; this was done in [61].

in these two cases are indistinguishable at any given angle of incidence, regardless of the number of layers. That is, the effective parameters corresponding to a single layer are the same as the bulk ones.

One may wonder why the main point of this section (one layer is already "bulk") has not been noted previously. There may be a general reason and a few incidental ones for that. Generally, homogenization of metamaterials is quite involved due to its non-asymptotic character [98]: to achieve unusual physical effects, the lattice cell size a can*not* be vanishingly small relative to the vacuum wavelength λ [93]. The complex field behavior in large lattice cells [$a \sim (0.2-0.4)\lambda$ in many cases of practical interest] tends to reduce the accuracy of homogenization; this is often interpreted as effects of spatial dispersion. Dependence of the effective parameters on the number of layers (or the absence of such dependence) is thereby obscured.

The incidental reasons alluded to above depend on the nature of research. Experimental work is likely to be affected by measurement errors and fabrication tolerances [91]. In analytical and numerical studies [14, 58, 78], dependence of the effective parameters on the number of layers has not been the main thrust of investigations and has not been studied in detail.

Since the above analysis relies in a principal way on periodicity and Bloch modes, the conclusions do not apply to random or pseudorandom structures, where considerations are qualitatively different.

VII Effective Medium Transformation

In standard effective medium theories, the type of the problem under consideration does not change upon homogenization. For example, a stationary heat transfer problem in a heterogeneous structure is, upon homogenization, still a heat transfer problem, with some effective parameters. Likewise, a wave problem remains a wave problem in an effective medium, even if the effective permeability turns from unity into a nontrivial value; and so on.

However, there is a peculiar case where homogenization changes qualitatively the character of the problem, both mathematical and physical. This has to do with eddy currents in stratified structures, typical for various types of electrical machines. To reduce induced currents and losses, magnetic cores are usually laminated: thin conducting magnetic sheets are coated with a thin layer of insulation, so that eddy currents are confined to the laminated sheets and cannot run across the whole magnetic core. As shown in [85], this eddy current problem becomes, under typical assumptions, mathematically a magneto-quasistatic one with a complex magnetic permeability. Here is a brief explanation of why this happens.

Consider cylindrical geometry typical for electric machines. The stratified structure is assumed to be infinite in the longitudinal (z) direction. Under this assumption, homogenization leads to fields and currents that cannot depend on z and do not have z-components. Then from the $\nabla \times \mathbf{H} = \mathbf{J}$ equation in the cylindrical system,[9] one has

$$J_z = 0$$
$$J_r = r^{-1}\partial_\phi H_z - \partial_z H_\phi = 0 - 0 = 0$$
$$J_\phi = \partial_z H_r - \partial_r H_z = 0 - 0 = 0 \quad (46)$$

[9] Displacement currents are neglected in the eddy current problem. This shows that in this setup eddy currents cannot be represented on the coarse scale, and the character of the problem has indeed changed qualitatively: eddy current equations have turned into magneto-quasistatic ones [85].

Acknowledgment

The article is based on my joint work with Vadim Markel, Shahriyar Hossain, Markus Schöbinger, Karl Hollaus, and Yidong Chong. Research projects with Vadim Markel and Shahriyar Hossain were supported in part by the US National Science Foundation awards DMS-1216970 and DMS-1620112. The work of Karl Hollaus and Markus Schöbinger was supported in part by the Austrian Science Fund (FWF) under Project P 31926, and Yidong Chong's research – by the Singapore MOE Academic Research Fund Tier 3 Grant MOE2016-T3-1-006.

I thank Alain Bossavit, Graeme Milton, Ralf Hiptmair, Sergey Bozhevolnyi, Anders Pors, Andrei Lavrinenko, Radu Malureanu, Carsten Rockstuhl, Che-Ting Chan, Xiaoyan Xiong, Li Jun Jiang, Stéphane Clénet, Joachim Schöberl for many interesting discussions.

Special thanks to Peter Bermel and Ze Wang (Purdue University) for their help with S^4/nanohub simulations.

Finally, I am grateful to Kay Hameyer and Jan Sykulski for the opportunity to contribute to the Compumag Society newsletter.

VIII References

[1] Assyr Abdulle, E Weinan, Björn Engquist, and Eric Vanden-Eijnden. The heterogeneous multiscale method. *Acta Numerica*, 21:1–87, 2012.

[2] Andrei Andryieuski, Andrei V Lavrinenko, and Sergei V Zhukovsky. Anomalous effective medium approximation breakdown in deeply subwavelength all-dielectric photonic multilayers. *Nanotechnology*, 26(18):184001, Apr 2015.

[3] N. S. Bakhvalov and G. Panasenko. *Homogenisation: Averaging Processes in Periodic Media, Mathematical Problems in the Mechanics of Composite Materials*. Springer, 1989.

[4] S. Bassiri, C. H. Papas, and N. Engheta. Electromagnetic wave propagation through a dielectric–chiral interface and through a chiral slab. *J. Opt. Soc. Am. A*, 5(9):1450–1459, Sep 1988.

[5] A. Bensoussan, J.L. Lions, and G. Papanicolaou. *Asymptotic Methods in Periodic Media*. North Holland, 1978.

[6] A. J. Bergqvist and S. G. Engdahl. A homogenization procedure of field quantities in laminated electric steel. *IEEE Trans Magn*, 37(5, 1):3329–3331, SEP 2001. 9th Biennial IEEE Conference on Electromagnetic Field Computation (CEFC), Milwaukee, Wisconsin, June 04–07, 2000.

[7] Alfredo Bermudez, Dolores Gomez, and Pilar Salgado. Eddy-current losses in laminated cores and the computation of an equivalent conductivity. *IEEE Trans Magn*, 44(12):4730–4738, Dec 2008.

[8] Craig F. Bohren. Light scattering by an optically active sphere. *Chemical Physics Letters*, 29(3):458–462, 1974.

[9] A. Bossavit, G. Griso, and B. Miara. Modelling of periodic electromagnetic structures bianisotropic materials with memory effects. *J. Math. Pures & Appl.*, 84(7):819–850, 2005.

[10] Oriano Bottauscio, Mario Chiampi, and Alessandra Manzin. Computation of higher order spatial derivatives in the multiscale expansion of electromagnetic-field problems. *IEEE Trans Magn*, 44(6):1194–1197, June 2008. 16th Biennial Compumag Conference on Computation of Electromagnetic Fields, Aachen, Germany, June 24–28, 2007.

[11] Oriano Bottauscio and Alessandra Manzin. Comparison of multiscale models for eddy current computation in granular magnetic materials. *Journal of Computational Physics*, 253:1–17, Nov 15 2013.

[12] Oriano Bottauscio, Alessandra Manzin, Valeria Chiado Piat, Marco Codegone, and Mario Chiampi. Electromagnetic phenomena in heterogeneous media: Effective properties and local behavior. *Journal of Applied Physics*, 100(4), Aug 15 2006.

[13] A. V. Chebykin, A. A. Orlov, C. R. Simovski, Yu. S. Kivshar, and P. A. Belov. Nonlocal effective parameters of multilayered metal-dielectric metamaterials. *Phys. Rev. B*, 86:115420, Sep 2012.

[14] X. Chen, T. M. Grzegorczyk, B.-I. Wu, J. Pacheco, and J. A. Kong. Robust method to retrieve the constitutive effective parameters of metamaterials. *Phys. Rev. E*, 70:016608, 2004.

[15] Zhiguang Cheng, Norio Takahashi, and Behzad Forghani. TEAM Problem 21 Family (V.2009). 2009. Approved by the International Compumag Society Board at Compumag-2009, Florianópolis, Brazil.

[16] Ruey-Lin Chern. Spatial dispersion and nonlocal effective permittivity for periodic layered metamaterials. *Opt. Express*, 21(14):16514–16527, Jul 2013.

[17] Tuck C. Choy. *Effective Medium Theory: Principles and Applications*. Oxford University Press, 1999.

[18] M Clemens, S Feigh, and T Weiland. Geometric multigrid algorithms using conformal finite integration technique. *IEEE Trans Magn*, 40(2, 2):1065–1068, Mar 2004. 14th Annual Conference on the Computation of Electromagnetic Fields (COMPUMAG 2003), Saratoga Springs, NY, July 13–17, 2003.

[19] Romain Corcolle, Xiaotao Ren, and Laurent Daniel. Effective properties and eddy current losses of soft magnetic composites. *Journal of Applied Physics*, 129(1), Jan 7 2021.

[20] H De Gersem and K Hameyer. Full multigrid for magnetostatics using unstructured and non-nested meshes. *IEEE Trans Magn*, 37(5, 1):3460–3464, Sep 2001. 9th Biennial IEEE Conference on Electromagnetic Field Computation (CEFC), Milwaukee, Wisconsin, June 04–07, 2000.

[21] Weinan E, Bjorn Engquist, Xiantao Li, Weiqing Ren, and Eric Vanden-Eijnden. Heterogeneous multiscale methods: A review. *Comm Comp Phys*, 2(3):367–450, 2007.

[22] M ElFeddi, Z Ren, A Razek, and A Bossavit. Homogenization technique for Maxwell equations in periodic structures. *IEEE Trans Magn*, 33(2, 2):1382–1385, Mar 1997. 7th Biennial IEEE Conference on Electromagnetic Field Computation (IEEE CEFC 96), Okayama, Japan, Mar 18–20, 1996.

[23] N. Engheta and D. L. Jaggard. Electromagnetic chirality and its applications. *IEEE Antennas and Propagation Society Newsletter*, 30(5):6–12, October 1988.

[24] J. Fish and V. Belsky. Multigrid method for periodic heterogeneous media. 2. multiscale modeling and quality-control in multidimensional case. *Comp Meth Appl Mech Eng*, 126(1–2):17–38, 1995.

[25] Szabolcs Gyimothy, Anett Kenderes, Sandor Bilicz, Jozsef Pavo, and Zsolt Badics. Homogenized 3-d FEM model for simulation of HTS coils. 2019. 22nd International Conference on the Computation of Electromagnetic Fields (COMPUMAG), Sorbonne Univ, Paris, France, July 15–19, 2019.

[26] J. Gyselinck and X. M. Lopez-Fernandez. Frequency and time domain homogenization of laminated magnetic cores and windings in fe models of high-frequency electromagnetic devices. *COMPEL – The International Journal for Computation and Mathematics in Electrical and Electronic Engineering*, 25(4):779–791, 2006.

[27] J Gyselinck, RV Sabariego, and P Dular. A nonlinear time-domain homogenization technique for laminated iron cores in three-dimensional finite-element models. *IEEE Trans Magn*, 42(4):763–766, April 2006. 15th Biennial Conference on Computation of Electromagnetic Fields, Shenyang, China, June 26–30, 2005.

[28] Johan Gyselinck, Patrick Dular, Laurent Kraehenbuehl, and Ruth V. Sabariego. Finite-element homogenization of laminated iron cores with inclusion of net circulating currents due to imperfect insulation. *IEEE Trans Magn*, 52(3), March 2016. 20th International Conference on the Computation of Electromagnetic Fields (Compumag), McGill Univ, Montreal, Canada, June 28 – July 02, 2015.

[29] T Hanawa, S Ikuno, and A Kamitani. Application of parallelized multigrid method to solution of mhd equilibrium with mpi. *IEEE Trans Magn*, 40(2, 2):1005–1008, March 2004. 14th Annual Conference on the Computation of Electromagnetic Fields (COMPUMAG 2003), Saratoga Springs, NY, July 13–17, 2003.

[30] Valentin Hanser, Markus Schöbinger, and Karl Hollaus. Efficient computation of eddy current losses in laminated cores with air gaps by the multiscale fem. In *2022 23rd International Conference on the Computation of Electromagnetic Fields (COMPUMAG)*, pages 1–4, 2022.

[31] Hanan Herzig Sheinfux, Ido Kaminer, Yonatan Plotnik, Guy Bartal, and Mordechai Segev. Subwavelength multilayer dielectrics: Ultrasensitive transmission and breakdown of effective-medium theory. *Phys. Rev. Lett.*, 113:243901, Dec 2014.

[32] Nabil Hihat, Ewa Napieralska-Juszczak, Jean-Philippe Lecointe, Jan K. Sykulski, and Krzysztof Komeza. Equivalent permeability of step-lap joints of transformer cores: Computational and experimental considerations. *IEEE Trans Magn*, 47(1):244–251, 2011.

[33] V Hill, O Farle, and R Dyczij-Edlinger. Finite element basis functions for nested meshes of nonuniform refinement level. *IEEE Trans Magn*, 40(2, 2):981–984, March 2004. 14th Annual Conference on the Computation of Electromagnetic Fields (COMPUMAG 2003), Saratoga Springs, NY, July 13-17, 2003.

[34] K. Hollaus and J. Schöberl. Some 2-d multiscale finite-element formulations for the eddy current problem in iron laminates. *IEEE Trans Magn*, 54(4), April 2018.

[35] Karl Hollaus and Joachim Schöberl. Multi-scale fem and magnetic vector potential a for 3d eddy currents in laminated media. *COMPEL – The International Journal for Computation and Mathematics in Electrical and Electronic Engineering*, 34(5, SI):1598–1608, 2015. 14th International IGTE Symposium on Numerical Field Calculation in Electrical Engineering (IGTE), Graz, Austria, September 2010.

[36] Karl Hollaus and Markus Schöbinger. A mixed multiscale fem for the eddy-current problem with t, phi-phi in laminated conducting media. *IEEE Trans Magn*, 56(4), April 2020.

[37] A. N. M. Shahriyar Hossain, Igor Tsukerman, and Vadim A. Markel. Homogenization of periodic structures: One layer is "bulk". *Europhysics Letters*, 138(3):35001, May 2022.

[38] ANM Hossain. Metamaterials: 3-D Homogenization and Dynamic Beam Steering. Master's thesis, The University of Akron, 2019.

[39] A.N.M. Shahriyar Hossain and Igor Tsukerman. Nonasymptotic homogenization of 3-d periodic structures. *Physics Letters A*, 398:127278, 2021.

[40] Thomas Y. Hou, Xiao-Hui Wu, and Zhiqiang Cai. Convergence of a multiscale finite element method for elliptic problems with rapidly oscillating coefficients. *Math of Comp*, 68(227):913–943, 1999.

[41] Xue Jiang and Weiying Zheng. Homogenization of quasi-static Maxwell's equations. *Multiscale Modeling & Simulation*, 12(1):152–180, 2014.

[42] V.V. Jikov, S.M. Kozlov, and O.A. Oleinik. *Homogenization of Differential Operators and Integral Functionals*. Springer-Verlag: Berlin ; New York, 1994.

[43] M Kaltenbacher, H Landes, S Reitzinger, and R Peipp. 3-d simulation of electrostatic-mechanical transducers using algebraic multigrid. *IEEE Trans Magn*, 38(2, 1):985–988, March 2002. 13th Annual Conference on the Computation of Electromagnetic Field (COMPUMAG 01), Evian Les Bains, France, July 02–05, 2001.

[44] Jiarui Kang, Xufeng Wang, Peter Bermel, and Chang Liu. S4: Stanford Stratified Structure Solver.

[45] N. A. Khizhnyak. Artificial anisotropic dielectrics: I. Artificial anisotropic dielectrics: II. Artificial anisotropic dielectrics: III. *Sov. Phys. Tech. Phys.*, 27:2006–2013, 2014–2026, 2027–2037, 1957.

[46] N. A. Khizhnyak. Artificial anisotropic dielectrics formed from two-dimensional lattices of infinite bars and rods. *Sov. Phys. Tech. Phys.*, 29:604–614, 1959.

[47] Jacob B. Khurgin. How to deal with the loss in plasmonics and metamaterials. *Nature Nanotechnology*, 10(1):2–6, Jan 2015.

[48] J. A. Kong. Optics of bianisotropic media. *Journal of the Optical Society of America*, 64(10):1304–1308, 1974.

[49] Christian Kruettgen, Simon Steentjes, Gregor Glehn, and Kay Hameyer. Parametric homogenized model for inclusion of eddy currents and hysteresis in 2-d finite-element simulation of electrical machines. *IEEE Trans Magn*, 53(6), June 2017.

[50] D.-H. Kwon, D. H. Werner, A. V. Kildishev, and V. M. Shalaev. Material parameter retrieval procedure for general bi-isotropic metamaterials and its application to optical chiral negative-index metamaterial design. *Opt. Express*, 16:11822, 2008.

[51] D Lahaye, H De Gersem, S Vandewalle, and K Hameyer. Algebraic multigrid for complex symmetric systems. *IEEE Trans Magn*, 36(4, 1):1535–1538, July 2000. 12th Conference on the Computation of Electromagnetic Fields (COMPUMAG 99), Sapporo, Japan, Oct 25-28, 1999.

[52] A. Lakhtakia and W.S. Weiglhofer. Lorentz covariance, Occam's razor, and a constraint on linear constitutive relations. *Physics Letters A*, 213:107–111, 1996.

[53] Akhlesh Lakhtakia. Boundary-value problems and the validity of the Post constraint in modern electromagnetism. *Optik*, 117(4):188–192, 2006.

[54] Xinrui Lei, Lei Mao, Yonghua Lu, and Pei Wang. Revisiting the effective medium approximation in all-dielectric subwavelength multilayers: Breakdown and rebuilding. *Phys. Rev. B*, 96:035439, Jul 2017.

[55] L. Lewin. The electrical constants of a material loaded with spherical particles. *Proc. Inst. Elec. Eng.*, 94:65–68, 1947.

[56] Victor Liu and Shanhui Fan. S4: A free electromagnetic solver for layered periodic structures. *Comput Phys Comm*, 183(10):2233–2244, 2012.

[57] Yan Liu, Sébastien Guenneau, and Boris Gralak. Artificial dispersion via high-order homogenization: magnetoelectric coupling and magnetism from dielectric layers. *Proc. R. Soc. A*, 469:2013.0240, 2013.

[58] Guang Lu, Feng Wu, Minjia Zheng, Chaoxin Chen, Xiachen Zhou, Chao Diao, Fen Liu, Guiqiang Du, Chunhua Xue, Haitao Jiang, and Hong Chen. Perfect optical absorbers in a wide range of incidence by photonic heterostructures containing layered hyperbolic metamaterials. *Opt. Express*, 27(4):5326–5336, Feb 2019.

[59] Shampy Mansha, Igor Tsukerman, and Yidong Chong. The FLAME-slab method for electromagnetic wave scattering in aperiodic slabs. *Optics Express*, 25:32602–32617, 2017.

[60] Vadim A. Markel and John C. Schotland. Homogenization of Maxwell's equations in periodic composites: Boundary effects and dispersion relations. *Phys. Rev. E*, 85:066603, Jun 2012.

[61] Vadim A. Markel and Igor Tsukerman. Current-driven homogenization and effective medium parameters for finite samples. *Phys. Rev. B*, 88:125131, Sep 2013.

[62] Gerard Meunier, Vincent Charmoille, Christophe Guerin, Patrice Labie, and Yves Marechal. Homogenization for periodical electromagnetic structure: Which formulation? *IEEE Trans Magn*, 46(8):3409–3412, Aug 2010. 17th International Conference on the Computation of Electromagnetic Fields (COMPUMAG 09), Florianopolis, Brazil, Nov 22–26, 2009.

[63] M. G. Moharam and T. K. Gaylord. Rigorous coupled-wave analysis of planar-grating diffraction. *J. Opt. Soc. Am.*, 71(7):811–818, Jul 1981.

[64] M. G. Moharam, Drew A. Pommet, Eric B. Grann, and T. K. Gaylord. Stable implementation of the rigorous coupled-wave analysis for surface-relief gratings: enhanced transmittance matrix approach. *J. Opt. Soc. Am. A*, 12(5):1077–1086, May 1995.

[65] Cesar Monzon and D. W. Forester. Negative refraction and focusing of circularly polarized waves in optically active media. *Phys. Rev. Lett.*, 95:123904, Sep 2005.

[66] Alexander Moroz. Effective medium properties, mean-field description, homogenization, or homogenisation of photonic crystals. http://www.wave-scattering.com/pbgheadlines.html.

[67] N. Neuss, W. Jager, and G. Wittum. Homogenization and multigrid. *Computing*, 66(1):1–26, 2001.

[68] Korawich Niyomsatian, Johan Gyselinck, and Ruth V. Sabariego. Closed-form complex permeability expression for proximity-effect homogenisation of litz-wire windings. *IET Science Measurement & Technology*, 14(3):287–291, May 2020.

[69] I. Niyonzima, R. V. Sabariego, P. Dular, F. Henrotte, and C. Geuzaine. Computational homogenization for laminated ferromagnetic cores in magnetodynamics. *IEEE Trans Magn*, 49(5):2049–2052, May 2013. 15th Biennial IEEE Conference on Electromagnetic Field Computation (CEFC), Oita, Japan, Nov 11–14, 2012.

[70] I. Niyonzima, R. V. Sabariego, P. Dular, K. Jacques, and C. Geuzaine. Multiscale finite element modeling of nonlinear magnetoquasistatic problems using magnetic induction conforming formulations. *Multiscale Modeling & Simulation*, 16(1):300–326, 2018.

[71] Paul Penfield and H. A. Haus. *Electrodynamics of Moving Media*. The MIT Press, 1967.

[72] Guanghua Peng, R. Dyczij-Edlinger, and Jin-Fa Lee. Hierarchical methods for solving matrix equations from TVFEMs for microwave components. *IEEE Trans Magn*, 35(3, 1):1474–1477, May 1999. 8th Biennial IEEE Conference on Electromagnetic Field Computation (IEEE CEFC 98), Tucson, AZ, June 01–03, 1998.

[73] A. Plaks, I. Tsukerman, G. Friedman, and B. Yellen. Generalized Finite Element Method for magnetized nanoparticles. *IEEE Trans. Magn.*, 39(3):1436–1439, 2003.

[74] A. Plaks, I. Tsukerman, S. Painchaud, and L. Tabarovsky. Multigrid methods for open boundary problems in geophysics. *IEEE Trans. Magn.*, 36(4):633–638, 2000.

[75] Gisela Poeplau and Ursula van Rienen. A self-adaptive multigrid technique for 3-d space charge calculations. *IEEE Trans Magn*, 44(6):1242–1245, June 2008. 16th Biennial COMPUMAG Conference on Computation of Electromagnetic Fields, Aachen, Germany, June 24–28, 2007.

[76] G Poplau, U van Rienen, B van der Geer, and M de Loos. Multigrid algorithms for the fast calculation of space-charge effects in accelerator design. *IEEE Trans Magn*, 40(2, 2):714–717, March 2004. 14th Annual Conference on the Computation of Electromagnetic Fields (COMPUMAG 2003), Saratoga Springs, NY, July 13–17, 2003.

[77] Vladislav Popov, Andrei V. Lavrinenko, and Andrey Novitsky. Operator approach to effective medium theory to overcome a breakdown of Maxwell Garnett approximation. *Phys. Rev. B*, 94:085428, Aug 2016.

[78] Anders Pors, Igor Tsukerman, and Sergey I. Bozhevolnyi. Effective constitutive parameters of plasmonic metamaterials: Homogenization by dual field interpolation. *Phys Rev E*, 84:016609, 2011.

[79] R J Potton. Reciprocity in optics. *Reports on Progress in Physics*, 67(5):717–754, Apr 2004.

[80] Ilia L. Rasskazov, Sergei V. Karpov, and Vadim A. Markel. Waveguiding properties of short linear chains of nonspherical metal nanoparticles. *J. Opt. Soc. Am. B*, 31(12):2981–2989, Dec 2014.

[81] S Reitzinger, U Schreiber, and U van Rienen. Electroquasi static calculation of electric field strength on high-voltage insulators with an algebraic multigrid algorithm. *IEEE Trans Magn*, 39(4, 2):2129–2132, July 2003. 10th IEEE Biennial Conference on Electromagnetic Field Computation (CEFC 02), Perugia, Italy, Jun 16-19, 2002.

[82] Xiaotao Ren, Romain Corcolle, and Laurent Daniel. A homogenization technique to calculate eddy current losses in soft magnetic composites using a complex magnetic permeability. *IEEE Trans Magn*, 52(12):1–9, 2016.

[83] E. Sanchez-Palencia. *Non-homogeneous Media and Vibration Theory*. Springer Verlag, 1980.

[84] Yuki Sato and Hajime Igarashi. Homogenization method based on model order reduction for fe analysis of multi-turn coils. 2016. 17th IEEE Biennial Conference on Electromagnetic Field Computation (IEEE CEFC), Miami, FL, Nov 13–16, 2016.

[85] Markus Schöbinger, Igor Tsukerman, and Karl Hollaus. Effective medium transformation: The case of eddy currents in laminated iron cores. *IEEE Trans Magn*, 57(11):6302506, 2021.

[86] M. G. Silveirinha. Metamaterial homogenization approach with application to the characterization of microstructured composites with negative parameters. *Physical Review B*, 75(11):115104, 2007.

[87] C. R. Simovski. Material paremeters of metamaterials (a review). *Optics and Spectroscopy*, 107(5):766–793, 2009.

[88] C. R. Simovski. On electromagnetic characterization and homogenization of nanostructured metamaterials. *Journal of Optics*, 13:103001, 2011.

[89] Daniel Sjöberg, Christian Engstrom, Gerhard Kristensson, David J. N. Wall, and Niklas Wellander. A Floquet–Bloch decomposition of maxwell's equations applied to homogenization. *Multiscale Modeling & Simulation*, 4(1):149–171, 2005.

[90] D.R. Smith, S. Schultz, P. Markoš, and C.M. Soukoulis. Determination of effective permittivity and permeability of metamaterials from reflection and transmission coefficients. *Phys. Rev. B*, 65(19):195104, Apr 2002.

[91] Johneph Sukham, Osamu Takayama, Maryam Mahmoodi, Stanislav Sychev, Andrey Bogdanov, Seyed Hassan Tavassoli, Andrei V. Lavrinenko, and Radu Malureanu. Investigation of effective media applicability for ultrathin multilayer structures. *Nanoscale*, 11:12582–12588, 2019.

[92] Luc Tartar. *The General Theory of Homogenization: A Personalized Introduction*. Springer, 2009.

[93] Igor Tsukerman. Negative refraction and the minimum lattice cell size. *J. Opt. Soc. Am. B*, 25:927–936, 2008.

[94] Igor Tsukerman. Classical and non-classical effective medium theories: New perspectives. *Physics Letters A*, 381(19):1635–1640, 2017.

[95] Igor Tsukerman. *Computational Methods for Nanoscale Applications: Particles, Plasmons and Waves*. Springer, 2nd ed., 2020.

[96] Igor Tsukerman. Computational electromagnetics: A miscellany. *J*, 4(4):881–896, 2021. (Open access.).

[97] Igor Tsukerman, A. N. M. Shahriyar Hossain, and Y. D. Chong. Homogenization of layered media: Intrinsic and extrinsic symmetry breaking. *EPL (Europhysics Letters)*, 133(1):17003, Jan 2021.

[98] Igor Tsukerman and Vadim A. Markel. A nonasymptotic homogenization theory for periodic electromagnetic structures. *Proc Royal Society A*, 470:2014.0245, 2014.

[99] Igor Tsukerman and Alexander Plaks. Hierarchical basis multilevel preconditioners for 3d magnetostatic problems. *IEEE Trans. Magn.*, 35(3):1143–1146, 1999.

[100] Igor Tsukerman and Alexander Plaks. Refinement strategies and approximation errors for tetrahedral elements. *IEEE Trans. Magn.*, 35(3):1342–1345, 1999.

[101] Carlos A. Valdivieso, Gerard Meunier, Brahim Ramdane, Johan Gyselinck, Christophe Guerin, and Ruth V Sabariego. Time-domain finite-element eddy-current homogenization of windings using foster networks and recursive convolution. *IEEE Trans Magn*, 56(12), Dec 2020.

[102] G. Wasselynck, D. Trichet, B. Ramdane, and J. Fouldagar. Interaction between electromagnetic field and CFRP materials: A new multiscale homogenization approach. *IEEE Trans Magn*, 46(8):3277–3280, Aug 2010. 17th International Conference on the Computation of Electromagnetic Fields (COMPUMAG 09), Santa Catarina, Brazil, Nov 22–26, 2009.

[103] Kota Watanabe, Seiji Fujino, and Hajime Igarashi. Multigrid method with adaptive idr-based jacobi smoother. *IEEE Trans Magn*, 47(5):1210–1213, May 2011. 14th Biennial IEEE Conference on Electromagnetic Field Computation (CEFC), Chicago, IL, May 09–12, 2010.

[104] P. C. Waterman and N. E. Pedersen. Electromagnetic scattering by periodic arrays of particles. *J. Appl. Phys.*, 59:2609–2618, 1986.

[105] Xiaoyan Y.Z. Xiong, Li Jun Jiang, Vadim A. Markel, and Igor Tsukerman. Surface waves in three-dimensional electromagnetic composites and their effect on homogenization. *Optics Express*, 21(9):10412–10421, 2013.

[106] Pochi Yeh. *Optical Waves in Layered Media*. Hoboken, N.J.: John Wiley, 2005.

[107] Sergei V. Zhukovsky, Andrei Andryieuski, Osamu Takayama, Evgeniy Shkondin, Radu Malureanu, Flemming Jensen, and Andrei V. Lavrinenko. Experimental demonstration of effective medium approximation breakdown in deeply subwavelength all-dielectric multilayers. *Phys. Rev. Lett.*, 115:177402, Oct 2015.

Author's name and Affiliation

Igor Tsukerman, Department of Electrical and Computer Engineering, The University of Akron, OH 44325–3904, USA.

igor@uakron.edu